EL NIÑO AND LA NIÑA EFFECTS ON THE NORTHEAST PACIFIC: THE 1991–1993 AND 1988–1989 EVENTS

TOM MURPHREE
Department of Meteorology, MR/Me
Naval Postgraduate School
Monterey, California 93943-5114

CAROLYN REYNOLDS
Naval Research Laboratory
7 Grace Hopper Avenue, Stop 2
Monterey, California 93943-5502

ABSTRACT

The 1991–93 El Niño and 1988–89 La Niña events had substantial effects throughout the tropical Pacific Ocean and atmosphere. These events also greatly affected the extratropics, especially the northeastern Pacific region. A mechanism which appears to have been important in producing these effects was tropical atmospheric forcing of the mid-latitude atmosphere. This process caused shifts in the mid-latitude storm track over the North Pacific. These shifts led to marked changes in the wind forcing of the ocean, which apparently caused substantial ocean anomalies. Evidence for an additional teleconnection mechanism involving ocean Kelvin waves was found in the equatorial Pacific.

1. INTRODUCTION

Many studies have linked El Niño conditions in the tropical Pacific to low-frequency variations in the northeast Pacific atmosphere and ocean (e.g., Bjerknes 1972; Horel and Wallace 1981; Haney et al. 1983; Emery and Hamilton 1985; Mysak 1986; Namias 1986; Simpson 1992). The northeast Pacific variations that have received the greatest attention are anomalous seasonal-to-interannual fluctuations in atmospheric pressures, winds, and precipitation; in oceanic near-surface temperatures, salinities, and currents; and in sea levels. Most attention has been directed to fluctuations that occurred during and soon after the mature phase of El Niño events (Rassmusson and Carpenter 1982). These fluctuations are also thought to have large effects on many marine organisms. Such effects have created a great deal of interest in unravelling the physical processes by which El Niño events affect the extratropical northeast Pacific atmosphere and ocean (e.g., Glantz et al. 1991).

We review in this paper some of the major large-scale ocean and atmosphere processes that occurred during the 1991–93 El Niño and 1988–89 La Niña events, including their apparent effects on the extratropical northeast Pacific region. La Niña events, sometimes called anti-El Niño or cold events, produce effects in the northeast Pacific that tend to be the reverse of those during El Niño events. Comparisons of the 1991–93 El Niño and 1988–89 La Niña events provide useful insights into how the tropical ocean and atmosphere may affect the northeast Pacific region. The major features of these two events and their extratropical effects are good examples of what is typically observed during El Niño and La Niña events.

In the following sections, the 1991–93 event is presented primarily in terms of oceanic and atmospheric phenomena from January to June 1992, because the events during this period were representative of the major features and effects throughout the event.

2. DATA AND METHODS

We have used a variety of data from several sources for this study. The main data and their sources are:

1. daily mean equatorial Pacific Ocean temperatures, currents, and surface winds from the Tropical Ocean-Global Atmosphere (TOGA) moored buoy array in the equatorial Pacific (McPhaden 1993);
2. weekly mean sea-surface temperature (SST) analyses from the Climate Analysis Center of the National Meteorological Center[1];
3. monthly mean outgoing longwave radiation analyses from the Climate Analysis Center of the National Meteorological Center; and
4. daily mean global atmospheric geopotential height and wind analyses from the European Centre for Medium-range Weather Forecasts (ECMWF).

The ocean temperatures from the TOGA buoys were missing for a number of days. Also, the temperatures were not recorded at the same depths at all longitudes across the Pacific. Thus, we did some averaging and linear interpolation to fill in data gaps and produce time series at common depths.

We used the outgoing longwave radiation (OLR) data to estimate the location and intensity of tropical convective storms, and the latent heat released in those storms. The relationship of OLR to convective storms and latent heating of the atmosphere is based on the following reasoning. OLR represents the infrared radiation emitted to outer space by Earth. Thus OLR depends very strongly on the temperature of the region of Earth from which the emission occurs (Hartmann 1994). Areas

[1]Reynolds, R. W., and T. M. Smith. A high-resolution sea surface temperature climatology. MS submitted to J. Climate.

of strong tropical atmospheric convection (i.e., deep tropical storm systems) have tall clouds, with tops about 14–18 km above sea level. At these levels, cloud tops are quite cold, and OLR amounts from these convective systems are low.

Conversely, in tropical areas without strong convection, the levels that most effectively radiate to outer space are low lying and relatively warm (e.g., ocean, land, or low cloud tops). So the OLR from these surfaces is high. Since large amounts of latent heat are released in tropical convective systems, *low* OLR values indicate *high* latent heating of the tropical atmosphere, and vice versa. Latent heating in tropical convective systems is a very important process for driving the tropical and global atmosphere. So OLR is very useful for understanding the climate system and for diagnosing climate variations such as El Niño and La Niña events.

We used the geopotential height of the 200 mb surface to represent the atmosphere's dynamic topography near the top of the troposphere (8–18 km above sea level). Since horizontal variations in pressure force atmospheric motions, this topography can be used to infer upper-tropospheric winds.

Most of the data presented in this study are in the form of anomaly fields. We define an anomaly as the deviation of an individual time mean value from a multiyear mean value. For example, a wind anomaly for April 1992 is the mean wind for April 1992 minus the mean April wind of the past 14 years. The multiyear means used for the anomaly calculations varied with the data:

1. for SST, a blend of multiyear periods spanning 1950–93, with the exact period varying with the location and type of data[2]
2. for OLR, 1974–93
3. for geopotential heights and winds, 1980–93.

3. TROPICAL PROCESSES

a. El Niño and La Niña Events

El Niño and La Niña events are characterized by a complex set of anomalous physical conditions in the tropical Pacific Ocean and atmosphere. These anomalies occur on basinwide space scales and on seasonal to interannual time scales. Two anomalies of particular interest are those in tropical Pacific sea-surface temperature (SST) and OLR. These anomalies describe changes in the temporal and spatial distribution of thermal energy in the tropical ocean and atmosphere. These changes are important because the thermal energy of the tropics plays a major role in driving the climate system.

The thermal-energy disturbances that occur during El Niño and La Niña events are large, second only to normal seasonal changes (Peixoto and Oort 1992). Thus El Niño and La Niña thermal-energy changes may generate large disturbances around the globe. SST and OLR anomalies concisely represent these changes in the thermal energy of the tropical ocean and atmosphere. SST and OLR anomalies are also convenient to work with because there are extensive satellite observations from which SST and OLR can be readily calculated.

During El Niño events, the central and eastern tropical Pacific SST is higher than normal, and the OLR is lower than normal for several months or longer. During La Niña events, the SST and OLR anomaly patterns are similar but with opposite signs. Figure 1 shows representative examples of these anomalies during the 1991–93 El Niño and 1988–89 La Niña events. These anomalies are shown for the January-February-March (JFM) seasons of 1992 and 1989, when both the tropical anomalies and the extratropical responses to these anomalies tended to be largest. Note the general reversal between the El Niño and La Niña events of (a) the tropical Pacific SST and OLR anomalies, and (b) the extratropical North Pacific SST anomalies.

Good summaries of basic El Niño and La Niña processes and their relationship to other phenomena, such as the Southern Oscillation, are given by several authors (e.g., Philander 1990; Peixoto and Oort 1992).

b. Thermal Anomalies in the Tropical Ocean

SST anomalies (SSTAs) are an important and very commonly used indicator of anomalous ocean processes and air-sea heat exchange. But for processes and exchanges occurring on intraseasonal to interannual time scales, anomalies in the temperature or heat content of the upper ocean (i.e., the layer above the main thermocline) may be more useful. Both of these anomalies are based on information about the vertical distribution of temperature between the surface and the main thermocline. Unfortunately, this information is only occasionally available for most parts of the ocean. However, in the equatorial Pacific, there is an array of moored buoys designed to monitor upper-ocean and surface-atmosphere conditions (McPhaden 1993).

Upper-ocean temperatures from this array during the 1991–93 El Niño event are shown in figure 2. The subsurface temperatures from the buoy at 0°N, 155°W (figure 2a) had an especially distinct signal during October 1991–April 1992. At about 125–150 m (the approximate thermocline depth), the temperatures at this buoy underwent large fluctuations of 5°–10°C over periods of about 40–60 days. Note that the onset of these large fluctuations coincided with a large rise in SST during October–December 1991 (figure 2a). The period of large

[2]Ibid.

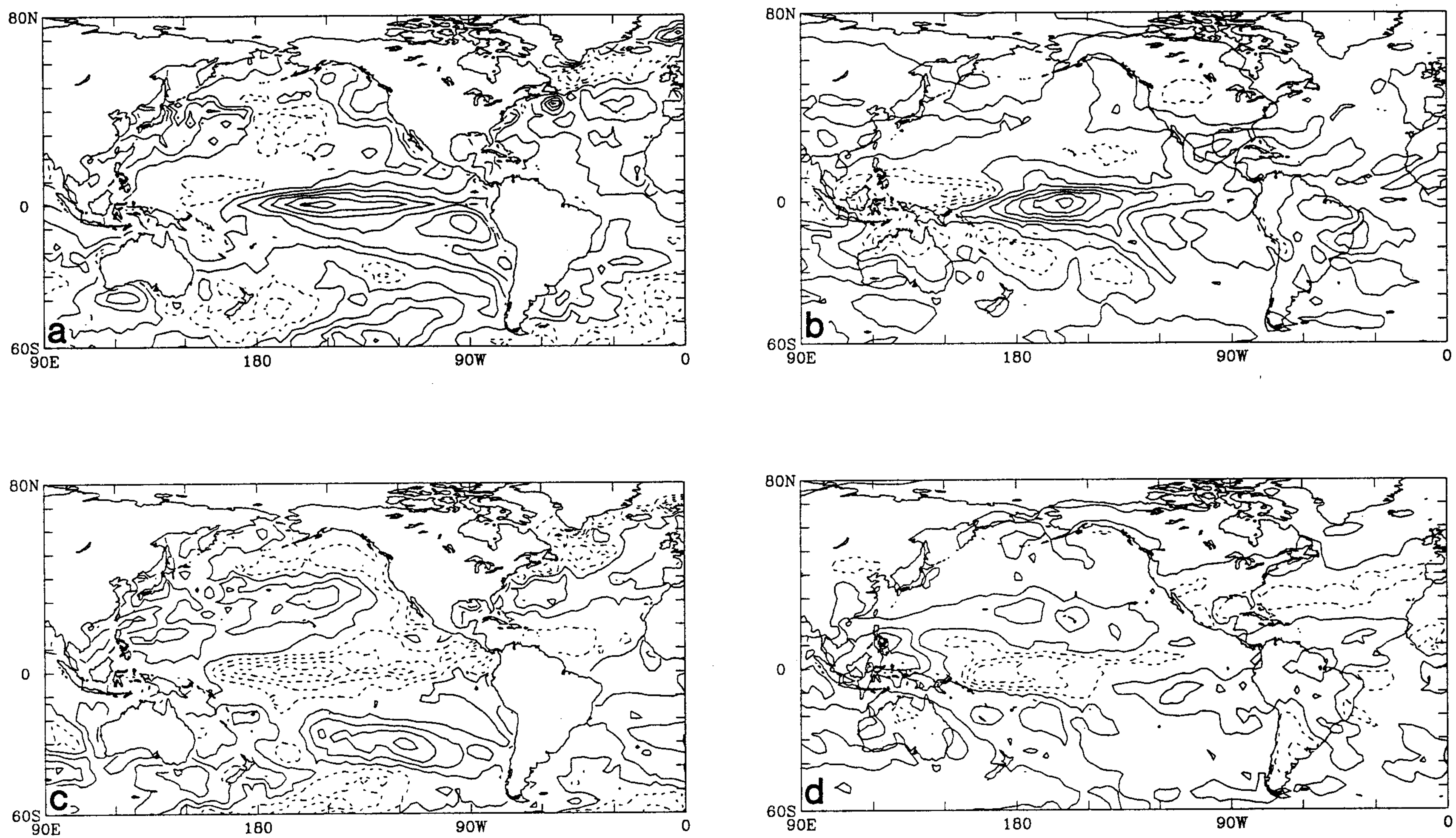

Figure 1. El Niño and La Niña sea-surface temperature anomalies (SSTAs) and outgoing longwave radiation anomalies (OLRAs) during the January-February-March (JFM) season. Negative (positive) OLRAs correspond to more-(less)-than-normal tropical convective storm activity, and more-(less)-than-normal latent heating of the tropical atmosphere. *a*, SSTA, JFM 1992; *b*, OLRA, JFM 1992; *c*, SSTA, JFM 1989; *d*, OLRA, JFM 1989. The SSTA contour interval is 0.5°C, with negative contours *dashed*. The OLRA contour interval is 10 Wm^{-2}, with positive contours *dashed*.

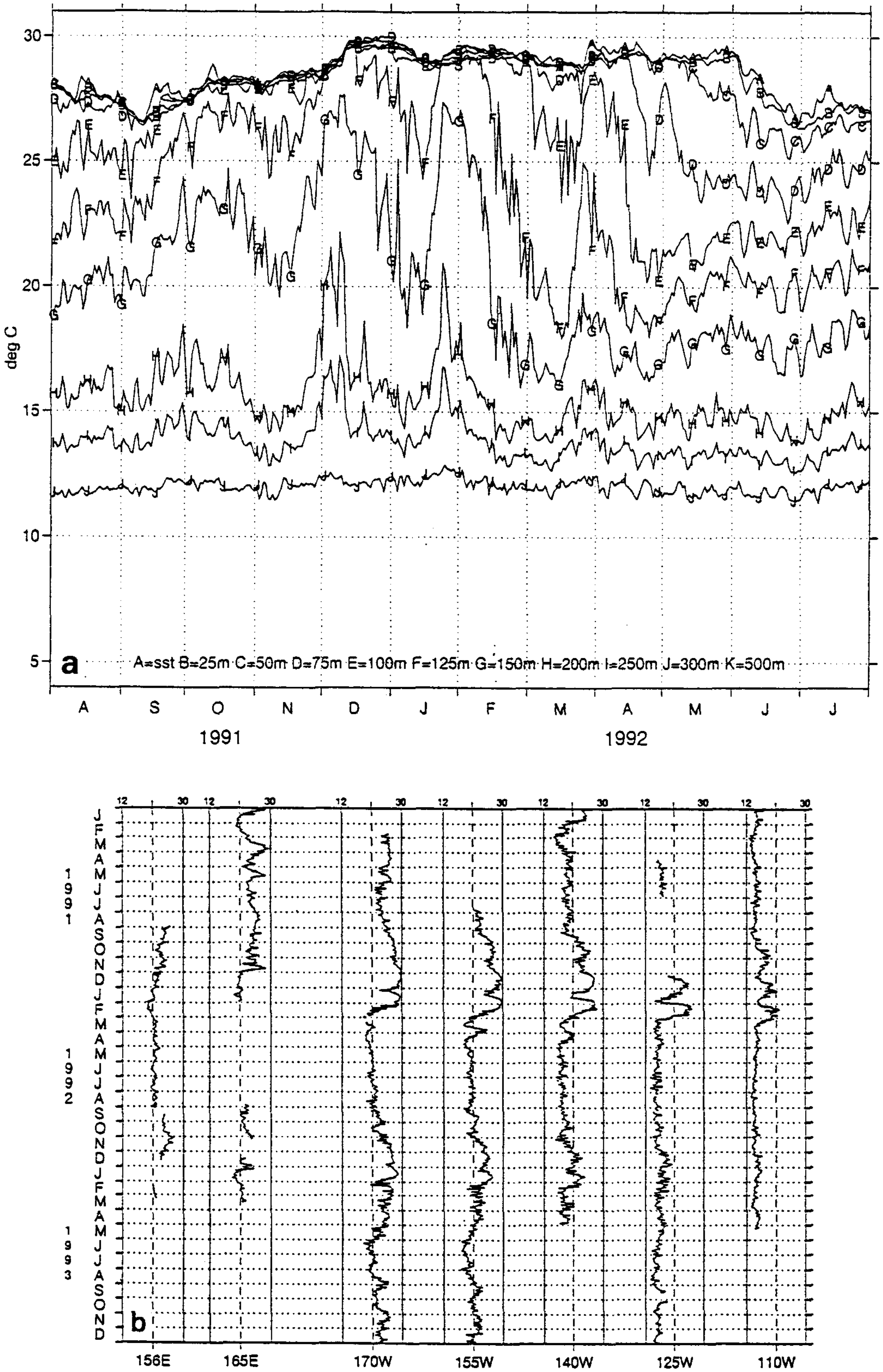

Figure 2. Ocean temperatures in the equatorial Pacific during the 1991–93 El Niño event. *a*, Temperatures at the equator and 155°W, 1 August 1991–31 July 1992, and from the surface to 500 m. Depths are indicated by the *letters* on the time series curves (key at the bottom of figure). *b*, Temperatures at 125 m along the equator at seven different longitudes, 1 January 1991–31 December 1993. For each longitude, the temperature scale range is 12°–30°C, marked by the *vertical lines* to the left and right of each time series.

subsurface fluctuations was also a time of warm SSTs (28°–30°C) and positive SSTAs (1°–2°C; figures 1a, 2a). Similar subsurface and surface temperature variations occurred at other central and eastern equatorial Pacific locations during October 1991–April 1992 and October 1992–April 1993 (figure 2b; McPhaden 1993).

The temporal and spatial patterns of these intraseasonal variations in upper-ocean temperature, along with current-velocity data (not shown), indicate internal equatorial ocean Kelvin waves (Kindle and Phoebus 1995; Murphree et al.[3]). Coriolis effects cause these waves to be confined within a few degrees of the equator and to propagate eastward along the equator (Gill 1982). The oscillatory motions within the waves produce horizontal convergence and divergence along the equator, which lead to downwelling and upwelling. The periods of especially warm subsurface temperatures in figure 2 indicate the passage of a downwelling Kelvin wave pulse. Note, as an example, the strong warming in the 125–200 m layer that occurred in late January–early February 1992 at 0°N, 155°W (figure 2a). The periods of especially cool subsurface temperatures represent the passage of upwelling pulses.

The eastward propagation of the 1991–93 Kelvin waves is indicated by the eastward shifts with time of the downwelling and upwelling phases, as shown in figure 2b. These shifts indicate eastward phase velocities of about 2.5 ms^{-1}, similar to those found in theoretical and modeling studies (e.g., Gill 1982; Geise and Harrison 1990; Kindle and Phoebus 1995). Correlations of the temperature time series in figure 2b with equatorial surface winds indicate that these Kelvin waves were initiated by eastward surface-wind anomalies, especially those associated with tropical cyclone winds, in the western Pacific.[4] Figure 2b shows that the major Kelvin wave activity occurred in October 1991–April 1992 and October 1992–April 1993. The SST and OLR anomalies were especially strong in the central and eastern tropical Pacific during these two periods (figure 1), indicating that these were the two mature phases of the 1991–93 El Niño event (Rassmusson and Carpenter 1982).

Ocean Kelvin waves are part of the process by which the tropical Pacific Ocean and atmosphere redistribute thermal energy and create anomalous SST and OLR patterns (Philander 1990). During El Niño events, equatorial ocean Kelvin waves play an important role in creating positive upper-ocean heat content anomalies in the central and eastern tropical Pacific (e.g., Graham and White 1988). These ocean anomalies, in turn, help create anomalies in tropical atmospheric convective activity—which may, in turn, enhance the ocean anomalies (e.g., Graham and White 1988; Philander 1992).

Equatorial ocean Kelvin waves may also play a role in producing some of the extratropical effects of El Niño and La Niña events. This may happen when the waves strike the coast of Ecuador and some of their energy propagates poleward, as coastal Kelvin waves, into the extratropics (Gill 1982). The changes in ocean temperature, salinity, flow, and sea level that occur during the passage of these waves may explain some of the anomalies observed in the extratropical northeast Pacific, especially very close to the west coast of North America (e.g., Enfield and Allen 1980; Chelton and Davis 1982; Clarke and Van Gorder 1994). This possibility is discussed further in section 7.

c. Thermal Anomalies in the Tropical Atmosphere

Thermal energy anomalies in the tropical atmosphere may be estimated from OLR anomalies (OLRAs). In JFM 1992, the central and eastern tropical Pacific OLRAs were negative and were located approximately over positive SSTAs (figures 1a, b). In JFM 1989, the OLRAs were positive and occurred over negative SSTAs (figure 1c, d). Persistent positive (negative) SSTAs during El Niño (La Niña) events tend to be associated with persistent positive (negative) tropospheric-heating anomalies. These associations occur because positive SSTAs tend to initiate and maintain atmospheric convection, whereas negative SSTAs suppress convection.

Tropospheric heating anomalies are thought to play a major role in producing the extratropical responses to El Niño and La Niña (Tribbia 1991). The anomalous tropical heating causes anomalies in the speed, direction, and convergence of lower-tropospheric tropical winds (e.g., the trade winds). These heating anomalies also cause anomalies in upward tropical convective winds and the divergence of upper-tropospheric tropical winds (Gill 1980). Anomalies in these tropical winds are linked to anomalies in extratropical winds through, in part, the anomalous advection of momentum and propagation of low-frequency atmospheric wave energy. This, in turn, leads to anomalies in the sea surface beneath these extratropical wind anomalies. These linkages are discussed further in sections 4 and 5.

4. EXTRATROPICAL EFFECTS

The extratropical effects of El Niño and La Niña events are generally easier to identify in the atmosphere than in the ocean. This is mainly because the atmosphere is much better observed and modeled than the ocean. Thus there is a *relatively* clear picture of how the extratropical atmosphere has responded in past events and might be expected to respond in future events.

[3]Murphree, T., J. Kent, and R. Gelaro. Interactions of equatorial ocean Kelvin waves and tropical cyclones during the 1991–1993 El Niño event. MS submitted to J. Geophys. Res.

[4]Ibid.

a. Anomalies in the Extratropical Atmosphere

Some of the clearest and most immediate of these effects are in the mid-latitude upper troposphere, at about 9–14 km above the surface, where the major jets affecting mid-latitude weather occur. The atmospheric pressure in this region is roughly 200 mb. So a map of the 200 mb height gives a good indication of the dynamic topography of the upper troposphere, and, by inference, the upper-tropospheric winds. The heating from tropical Pacific convective regions is especially important to the dynamic topography and winds over the North Pacific–North America (NPNA) region. Thus the shifts in the tropical convective heating that occur during El Niño and La Niña events tend to have large effects in the NPNA region (cf. Tribbia 1991; Hartmann 1994).

These effects are most easily seen in maps of the anomalous height of the 200 mb surface. Figure 3 shows the 200 mb height anomalies and the corresponding wind anomalies during the JFM seasons of 1992 and 1989. The H and L symbols in the height panels indicate high and low height anomalies. In JFM 1992, there was a high anomaly over Hawaii, a low over the mid-latitude northeast Pacific, a high over Canada, and a low near the east coast of the United States (figure 3a). In JFM 1989, there was a low centered southeast of Hawaii, a high centered just south of the Aleutians, a low over most of Canada and southern Greenland, and a high centered over the eastern United States (figure 3b). In both years, there were four main height-anomaly centers in the NPNA region, in roughly similar locations but with the anomaly signs during the El Niño year opposite to those during the La Niña year.

During JFM of 1992 and 1989, the center of the main tropical Pacific OLRA (figure 1b, d) occurred about 3000 km to the southwest of the simultaneous high in the 200 mb height anomaly near Hawaii (figure 3a, b). This is a typical relationship during El Niño and La Niña events. This relationship—along with the typical coincidence of the tropical Pacific SSTAs and OLRAs (figure 1) and the typical four-centers pattern of the NPNA height anomalies (figure 3)—indicates the dependence of the extratropical upper-tropospheric height anomalies on tropical heating anomalies. El Niño and La Niña 200 mb height anomalies are often interpreted as parts of a single phenomenon—a Rossby wave train—that was initiated by the tropical heating anomalies (e.g., Lau and Lim 1984; Chelliah et al. 1988; Tribbia 1991). This wave train represents the propagation of low-frequency wave energy out of the tropics and into the extratropics. In this interpretation, the El Niño–La Niña reversal of the extratropical 200 mb height-anomaly signs is due to the reversal in the tropical Pacific forcing (e.g., the reversals indicated by figure 1).

Both El Niño and La Niña events vary in their extratropical influence. But certain regions show characteristic El Niño and La Niña effects (Horel and Wallace 1981). One of the regions with relatively consistent effects is the NPNA area; the height anomalies in figure 3 are good examples of these effects. The pattern of high-low-high-low anomaly centers in the Hawaii-northeast Pacific-Canada-western North Atlantic locations is typical during the mature phase of El Niño events. The pattern of NPNA highs and lows shown in figure 3a is similar to the Pacific-North American (PNA) teleconnection pattern described by Wallace and Gutzler (1981).

The wind anomalies associated with the height anomalies in figure 3 are shown schematically by the arrows in that figure. The climatologic flow at 200 mb over the northeast Pacific is generally eastward (Peixoto and Oort 1992). The wind anomalies in this region during JFM 1992 (figure 3a) reveal that this eastward flow was unusually weak at about 45°N-55°N and unusually strong at about 20°N-35°N. This corresponds to an anomalous southward shift of the eastward upper-tropospheric jets. The reverse was true during JFM 1989 (figure 3b).

Such anomalies in jet flow are dynamically linked to anomalies in mid-latitude storms and their associated winds. In particular, periods and locations with anomalously strong northeast Pacific jets indicate more or stronger surface wind events of the type associated with large-scale mid-latitude storms (e.g., the typical winter and spring storms of the western United States). The surface winds in these storms are cyclonic (i.e., counterclockwise in the Northern Hemisphere).

The jet anomalies shown in figure 3 imply that cyclonic wind events occurred farther south than normal during JFM 1992, and farther north than normal during JFM 1989. During JFM 1992, this led to surface wind anomalies that were cyclonic over almost all of the extratropical North Pacific (figure 4a). This pattern was especially clear in the northeast Pacific, where, along most of the west coast of North America, the alongshore component was poleward. In JFM 1989, the anomalous winds were anticyclonic (i.e., clockwise in the Northern Hemisphere) across most of the extratropical North Pacific (figure 4b). Along the west coast of North America, between about 30°N and 60°N, the alongshore component was equatorward. The northeast Pacific surface wind anomalies shown in figure 4 are typical during El Niño and La Niña events (cf. Horel and Wallace 1981). This means that the actual surface winds along most of the U.S. west coast tend to have a weaker (stronger) than normal equatorward component during El Niño (La Niña) winters.

Figure 4 also shows the equatorial western and central Pacific surface wind anomalies discussed in section 3. The eastward anomalies during JFM 1992 and the westward anomalies in JFM 1989 played key roles in the

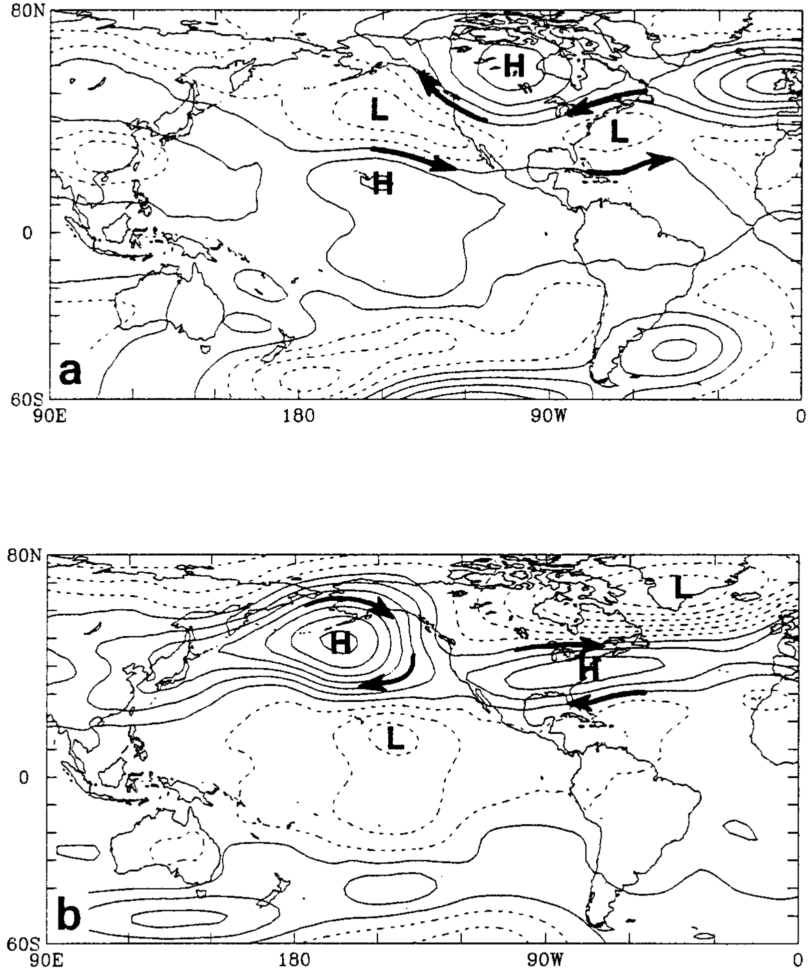

Figure 3. Atmospheric geopotential height and wind anomalies for the 200 mb surface during the January-February-March seasons of (*a*) 1992 and (*b*) 1989. Height anomaly contour interval is 30 geopotential meters, with negative contours *dashed*. Wind anomalies are shown schematically by *arrows* paralleling the height anomaly contours.

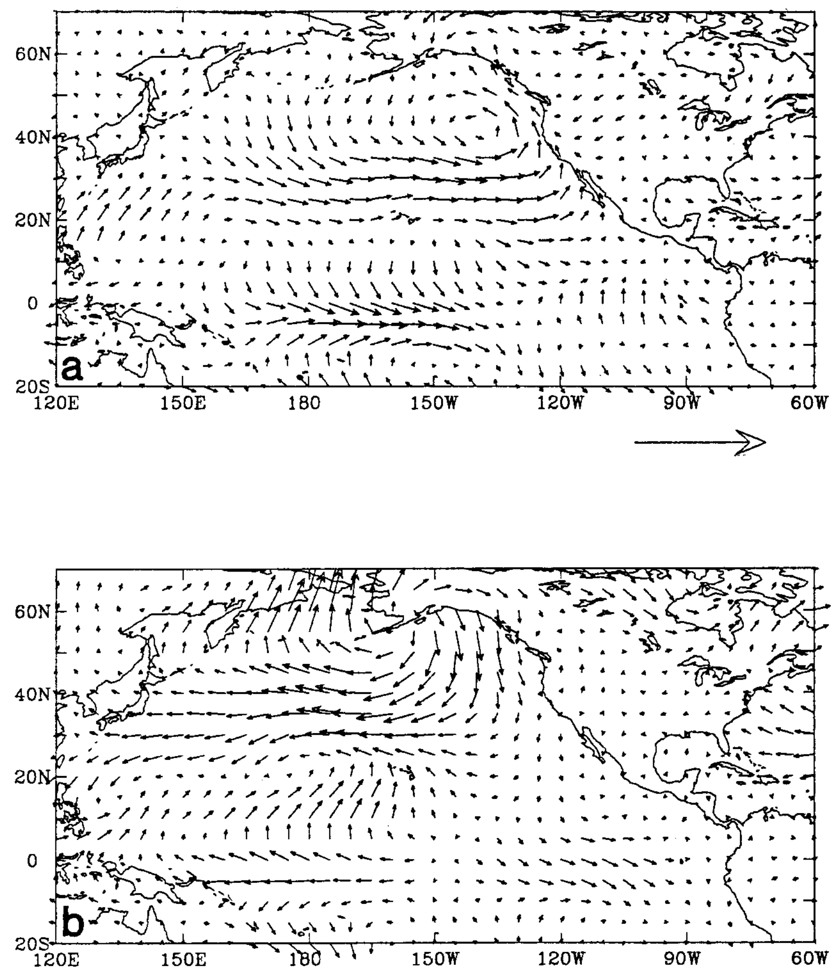

Figure 4. Surface wind anomalies during the January-February-March seasons of (*a*) 1992 and (*b*) 1989. Surface winds are represented by the *arrows* on the 1000 mb surface. The scale vector is shown at the bottom of panel *a* and represents 15 m s^{-1}.

development of the tropical SST and convective storm activity anomalies shown in figure 1.

b. Anomalies in the Extratropical Ocean

The extratropical surface wind anomaly patterns shown in figure 4 may have important effects on the extratropical ocean. Along the coast of California, the northward wind anomaly that is typical during an El Niño event has a poleward alongshore component that tends to produce anomalous decreases in offshore Ekman transport and upwelling. This produces anomalous increases in coastal sea level, SST, thermocline depth, and near-surface temperatures, plus anomalous decreases in equatorward flow. The long-term mean water-mass characteristics for the West Coast (Lynn et al. 1982) indicate that such coastal ocean circulation anomalies would also lead to anomalous decreases in salinities and increases in dissolved oxygen. These circulation, salinity, and oxygen anomalies, along with nutrient and biological anomalies, have been observed during past El Niño events (e.g., Wooster and Fluharty 1985; Mysak 1986; Breaker 1989; Simpson 1992; Lynn et al. 1995). For the 1991–93 event, Lynn et al. (1995) provide a detailed analysis of physical anomalies along the coast of California.

Ocean anomalies similar to those during El Niño events, but with opposite signs, tend to occur during La Niña events. For example, SST and sea-level anomalies along the west coast of North America have been observed to be positive (negative) during El Niño (La Niña) events (figure 1; Wyrtki 1989, 1992, 1993; Lynn et al. 1995). These ocean anomaly reversals are apparently linked to surface wind anomaly reversals such as those shown in figure 4.

5. VARIABILITY OF EXTRATROPICAL EFFECTS

A great deal of variability is embedded within the characteristic anomaly patterns described in sections 3 and 4. The duration and recurrence of El Niño and La Niña events shows some of this variability. Events tend to last about one year and recur at intervals of about three to seven years (Peixoto and Oort 1992). However, very different durations and intervals have been observed (e.g., Quinn et al. 1978; Diaz and Markgraf 1992). The 1991–93 event and its extratropical effects lasted about two years. Many tropical and extratropical aspects of the 1983–84 and 1988–89 La Niña events persisted into 1985 and 1990, respectively (e.g., Climate Analysis Center 1984, 1985; Kousky 1989, 1990; Bell and Halpert 1995).

The persistence of the 1991–93 event was somewhat unexpected, because the positive SSTAs and near-surface heat anomalies in the central and eastern equatorial Pacific had begun to decline by April 1992, and large areas of negative SSTAs occurred in that region throughout July–September 1992 (not shown). But in October 1992, the SSTAs there began to warm and continued to do so through about May 1993 (not shown).

Interseasonal variability during El Niño and La Niña events can be large. Such variability during the winter-to-spring transition can be especially important in the evolution of physical and biological anomalies in the northeast Pacific. Figure 5 shows the SST and surface wind anomalies for the April-May-June (AMJ) seasons of 1992 and 1989. A comparison of figure 1a with figure 5a shows that, from JFM to AMJ 1992, the negative SSTA in the central North Pacific and the positive SSTA along the west coast of North America intensified, except at about 45°N-50°N, where the positive SSTA weakened. Over the same period, the cyclonic surface wind anomaly in the northeast Pacific moved to the southwest, and the poleward wind anomalies along most of the west coast decreased (figures 4a and 5b).

The January–June 1989 changes over the North Pacific were dramatic. The positive SSTA in the western and central North Pacific weakened considerably, and the negative West Coast SSTA was replaced by a positive SSTA at about 20°N–60°N (figures 1c and 5c). The strong anticyclonic surface wind anomaly over southwest Alaska during JFM 1989 was drastically weakened and shifted eastward to the Gulf of Alaska (figures 4b and 5d).

The winter-to-spring changes in the SST and wind anomalies during 1991–93 and 1988–89 (figures 1, 4, 5) are representative of the wide range of interseasonal variability seen during individual El Niño and La Niña events. This range is similar to that seen at intraseasonal (e.g., month-to-month) scales (not shown).

6. PREDICTABILITY OF EXTRATROPICAL EFFECTS

Such variability from one event to the next and during an event makes predicting the extratropical effects difficult. Even small variations in key anomaly patterns may be significant. For example, relatively small changes in the location, orientation, and strength of the 200 mb height anomalies (section 4a) may lead to marked changes in the anomalies for the storm-track latitude, the speed of storms along the track, the angle between the track and the coast, the speed of the winds within the storms, and the location and amount of precipitation from the storms. These, in turn, may cause significant changes in mid-latitude air-sea interactions and ocean anomalies.

This sensitivity to small changes makes specific predictions of El Niño and La Niña events and their effects very problematic. For example, predictions of the location of the mid-latitude jet over the northeast Pacific for a particular week one month into the future are not reliable. This is due, in part, to the large internal variability of the mid-latitude atmosphere on such time scales.

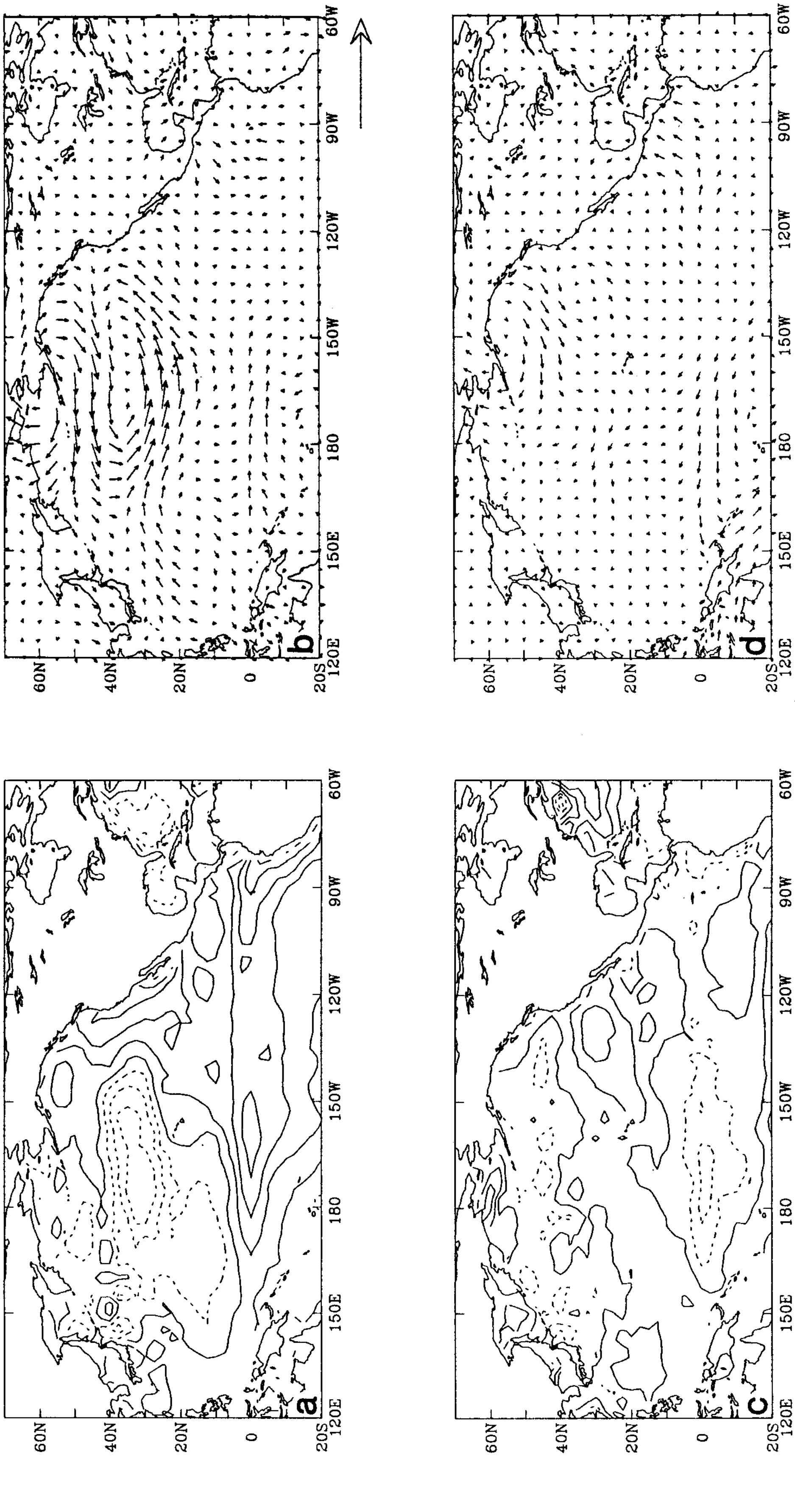

Figure 5. Sea-surface temperature anomaly (SSTA) and surface wind anomaly during the April-May-June (AMJ) seasons of 1992 and 1989. *a*, SSTA, AMJ 1992; *b*, wind anomaly, AMJ 1992; *c*, SSTA, AMJ 1989; *d*, wind anomaly, AMJ 1989. The SSTA contour interval is 0.5°C, with negative contours *dashed*. Surface winds are represented by the *arrows* on the 1000 mb surface. The scale vector is shown at the bottom of panel *b* and represents 15 m s^{-1}.

However, useful predictions may be made of the very large-scale and slowly varying anomalies related to El Niño and La Niña events (e.g., predictions of the broad-scale, seasonal 200 mb height-anomaly patterns, such as those shown in figure 3). Experimental predictions of El Niño and La Niña events and their effects are currently being made by several groups (e.g., Barnston 1994; Kumar and Hoerling 1995).

7. TELECONNECTION MECHANISMS

The El Niño and La Niña-driven interactions between the tropical Pacific and the extratropical northeast Pacific are examples of teleconnections, or interactions between widely separated parts of the environment. Most of the evidence for teleconnections forced by El Niño and La Niña events comes from observational time series correlation studies (e.g., Enfield and Allen 1980; Horel and Wallace 1981) and from modeling studies (e.g., Chelliah et al. 1988; Pares-Sierra and O'Brien 1989; Alexander 1992a, b; Clarke and Van Gorder 1994). The observational studies have established that there are a number of statistically significant teleconnections associated with El Niño and La Niña events. Both the observational and modeling studies have pointed toward two basic mechanisms that may explain how events in the tropics affect the extratropics. These mechanisms are, in essence:

1. the propagation of signals *through the atmosphere*, from the tropics into the extratropics, and then into the extratropical ocean
2. the propagation of signals *through the ocean*, from the tropics into the extratropics.

For both mechanisms, the primary propagating signal is the wave energy associated with large-scale, low-frequency waves—primarily Kelvin and Rossby waves (Gill 1982; Philander 1990). These waves play a key role in the adjustment of the ocean and atmosphere to El Niño and La Niña disturbances. As the thermal energy anomalies associated with El Niño and La Niña events evolve, the ocean and atmosphere adjust to the new distribution of thermal forcing by propagating wave energy away from the tropical Pacific disturbances.

Mechanism 1 involves the propagation of Rossby wave energy through the atmosphere (cf. section 4a). The observational and modeling evidence for this mechanism is, in general, good (e.g., Horel and Wallace 1981; Tribbia 1991). This is especially true for the broad-scale features of the atmospheric anomalies observed during El Niño or La Niña events. For example, the basic atmospheric anomaly patterns discussed in section 4a (e.g., the four upper-tropospheric height anomaly centers, the jet and storm-track shifts, the cyclonic and anticyclonic surface wind anomalies over the northeast Pacific) are explained by mechanism 1. This mechanism also explains the near-surface ocean anomalies that are driven by surface wind anomalies (see section 4).

But good support for this mechanism during *individual* El Niño or La Niña events has been more problematic (e.g., Chelliah et al. 1988). The primary reason is that Rossby waves are generated and affected by many processes other than El Niño or La Niña disturbances in the tropical Pacific. Thus, distinguishing the waves due to these other processes from those due to El Niño or La Niña effects is difficult. These other processes have also made it difficult to clearly identify the role of mechanism 1 in producing particular anomalies in an extratropical region.

However, as indicated in section 4, many regional anomalies are consistent with mechanism 1. The coastal sea-level and SST anomalies observed in the northeast Pacific are at least broadly consistent with the observed surface wind anomalies (section 4; Mysak 1986; Cayan 1992; Simpson 1992). These surface wind anomalies are linked to upper-tropospheric height anomalies that are consistent with a Rossby wave train emanating from a tropical Pacific heating anomaly (e.g., section 4a; Horel and Wallace 1981; Palmer and Mansfield 1986).

Mechanism 2 involves the propagation of ocean Kelvin waves eastward through the equatorial Pacific, and then poleward along the coasts of North America and South America (cf. section 3b). This mechanism also includes the possibility that westward-propagating ocean Rossby waves may be generated as the equatorial Kelvin waves strike the South American coast, and as the coastal Kelvin waves propagate along a coast with sharp changes in orientation (e.g., Gill 1982; White et al. 1989).

The equatorial Kelvin wave portion of mechanism 2 is well supported by observations, theory, and modeling (e.g., section 3b; Matsuno 1966; Gill 1980; Philander 1992). The poleward coastal Kelvin wave component of mechanism 2 is supported by some observations (especially coastal sea-level data; e.g., Enfield and Allen 1980; Chelton and Davis 1982) and by several modeling studies (e.g., Clarke and Van Gorder 1994; Jacobs et al. 1994). The TOGA array of moored buoys in the equatorial Pacific (McPhaden 1993) has provided much of the observational evidence for the equatorial part of mechanism 2. However, there is no comparable observation network for the eastern boundaries of the extratropical Pacific. That is, the relatively closely spaced (e.g., 2 degrees of latitude, 15 degrees of longitude) and frequent (e.g., hourly, daily) observations of the upper ocean and surface atmosphere that are available for the equatorial Pacific are missing for the coastal eastern Pacific. Thus the role of coastal Kelvin waves and associated Rossby waves in producing El Niño and La Niña teleconnections has been difficult to determine.

However, several aspects of the ocean anomalies discussed in section 4b are at least broadly consistent with mechanism 2. The northeast Pacific sea-level, current, and near-surface temperature anomalies associated with El Niño and La Niña events provide some evidence of poleward-propagating coastal Kelvin waves and westward-propagating Rossby waves (e.g., Enfield and Allen 1980; Chelton and Davis 1982; Jacobs et al. 1994; Norton and McClain 1994; Lynn et al. 1995).

Mechanisms 1 and 2 are not, of course, mutually exclusive. Both may be involved in producing the extratropical responses to El Niño and La Niña events, and the two mechanisms may interact with each other. For example, the extratropical surface wind anomalies that are part of mechanism 1 may well initiate coastal Kelvin waves and Rossby waves in the *extratropical* northeast Pacific (cf. Gill 1982). The extratropical near-surface ocean temperature anomalies that are part of mechanism 2 may influence the development of the overlying extratropical atmospheric pressures and winds that are part of mechanism 1.

8. DISCUSSION

We have examined the broad-scale features and effects of the 1991–93 El Niño and the 1988–89 La Niña events. These were relatively typical events in both their equatorial Pacific features and their extratropical effects (cf. Rassmusson and Carpenter 1982).

We have relied heavily in this study on monthly and seasonal anomalies. But such anomalies can be produced by several distinctly different series of events during the averaging period. For example, a number of mild storms off southern California during some March might cause a cyclonic surface wind anomaly for the month. But a couple of strong storms during a few days of the month, combined with otherwise weak winds could also cause such a cyclonic wind anomaly. Such differences in the *actual* wind events could, of course, lead to distinctly different monthly anomalies in ocean temperature, salinity, and flow—despite the similar monthly wind anomaly patterns.

Thus, although monthly and seasonal anomalies contain interesting patterns that reveal much about the workings of El Niño and La Niña events, they do not tell the whole story. In particular, they do not adequately address processes that occur at space and time scales that are smaller than those for which the monthly and seasonal anomalies were calculated. These unaddressed processes will be especially problematic in the study of ocean phenomena that have much smaller scales than the atmospheric anomalies. For example, attempting to interpret the variations of coastal eddies or comparably sized patches of marine organisms in terms of atmospheric anomalies may be very difficult because of scale mismatches.

These and other difficulties (see sections 6 and 7) would be well addressed by a more complete observational network (e.g., of moored buoys) in the northeast Pacific, especially along the eastern boundary. High-resolution satellite observations of SST, surface wind speeds, sea level, ocean color, and other ocean fields are available but have not been used much in exploring the effects of El Niño and La Niña on the northeast Pacific. The recent work by Strub and James (1995) gives an indication of how satellite-derived estimates of sea level might be used in concert with other satellite observations and on-site observations. Such satellite data should be very useful in resolving many of the present uncertainties about El Niño and La Niña effects.

ACKNOWLEDGMENTS

We wish to thank Ron Gelaro and Jeff Hawkins of the Naval Research Laboratory (NRL) in Monterey, California, for many helpful discussions and for their assistance in obtaining, displaying, and analyzing the ECMWF, SST, and OLR data. The Pacific Marine Environmental Laboratory provided the TOGA data. Grant Cooper, John Kent, and Todd Sitler—students at the Naval Postgraduate School—did much of the analysis of the TOGA data. The SST data were generously provided in a very accessible form by Dick Reynolds and Tom Smith at CAC. The OLR and ECMWF data were made available by CAC and ECMWF, by way of the National Center for Atmospheric Research. Leslie Rosenfeld of the Monterey Bay Aquarium Research Institute, Frank Schwing of the NOAA Pacific Fisheries Environmental Group, Dan Cayan of the Scripps Institution of Oceanography, and Patricia Phoebus of NRL provided very helpful suggestions for revisions of the original manuscript. This work was supported by NRL and the Office of Naval Research, Program Element 0601153N. Computing support was provided by the DoD High Performance Computing Program.

LITERATURE CITED

Alexander, M. A. 1992a. Midlatitude atmosphere-ocean interaction during El Niño. Part I: the North Pacific Ocean. J. Clim. 5:944–958.

———. 1992b. Midlatitude atmosphere-ocean interaction during El Niño. Part II: the Northern Hemisphere atmosphere. J. Clim. 5:959–972.

Barnston, A., ed. 1994. Experimental long-lead forecast bulletin, September 1994. Climate Analysis Center, National Oceanic and Atmospheric Administration, Washington, D.C. 37 pp.

Bell, G. D., and M. S. Halpert. 1995. Interseasonal and interannual variability: 1986–93. NOAA atlas no. 12. National Oceanic and Atmospheric Administration, Camp Springs, MD. 256 pp.

Bjerknes, J. 1972. Large-scale atmospheric response to the 1964–65 Pacific equatorial warming. J. Phys. Oceanogr. 2:212–217.

Breaker, L. 1989. El Niño and related variability in sea-surface temperature along the central California coast. Aspects of climate variability in the Pacific and western Americas. Am. Geophys. Union Geophys. Monogr. 55:133–140.

Cayan, D. R. 1992. Latent and sensible heat flux anomalies over the northern oceans. J. Clim. 5:354–369.

Chelliah, M., J. E. Schemm, and H. M. van den Dool. 1988. The effect of low-latitude anomalous forcing on local and remote circulation: winters 1978/79–1986/87. J. Clim. 1:1138–1152.

Chelton, D. B., and R. E. Davis. 1982. Monthly mean sea-level variability along the west coast of North America. J. Phys. Oceanogr. 12:757–784.

Clarke, A. J., and S. Van Gorder. 1994. On ENSO coastal currents and sea level. J. Phys. Oceanogr. 24:661–680.

Climate Analysis Center. 1984. Climate diagnostics bulletin, March 1984. Climate Analysis Center, National Meteorological Center, Washington, D.C. No. 84/4, 25 pp.

———. 1985. Climate diagnostics bulletin, March 1985. Climate Analysis Center, National Meteorological Center, Washington, D.C. No. 85/4, 45 pp.

Diaz, H. F., and V. Markgraf, eds. 1992. El Niño—historical and paleoclimatic aspects of the Southern Oscillation. New York: Cambridge Univ. Press, 476 pp.

Emery, W. J., and K. Hamilton. 1985. Atmospheric forcing of interannual variability in the northeast Pacific Ocean: connections with El Niño. J. Geophys. Res. 90:857–868.

Enfield, D. B., and J. S. Allen. 1980. On the structure and dynamics of monthly mean sea level anomalies along the Pacific coast of North and South America. J. Phys. Oceanogr. 10:557–578.

Geise, B. S., and D. E. Harrison. 1990. Aspects of the Kelvin wave response to episodic wind forcing. J. Geophys. Res. 95:7289–7312.

Gill, A. E. 1980. Some simple solutions for heat-induced tropical circulation. Quart. J. Royal Meteorol. Soc. 106:447–462.

———. 1982. Atmosphere-ocean dynamics. San Diego: Academic Press, 662 pp.

Glantz, M. H., R. W. Katz, and N. Nicholls, eds. 1991. Teleconnections linking worldwide climate anomalies: scientific basis and societal effects. New York: Cambridge Univ. Press, 535 pp.

Graham, N. E., and W. B. White. 1988. The El Niño cycle: a coupled oscillator of the Pacific Ocean-atmosphere system. Science 240:1293–1302.

Haney, R. L., B. H. Houtman, and W. H. Little. 1983. The relationship between wind and sea surface temperature anomalies in the midlatitude North Pacific Ocean. Atmos.-Ocean 21:168–186.

Hartmann, D. L. 1994. Global physical climatology. San Diego: Academic Press, 411 pp.

Horel, J., and J. M. Wallace. 1981. Planetary-scale atmospheric phenomena associated with the Southern Oscillation. Monthly Weather Rev. 109: 813–829.

Jacobs, G. A., H. E. Hurlburt, J. C. Kindle, E. J. Metzger, J. L. Mitchell, W. J. Teague, and A. J. Wallcraft. 1994. Decade-scale trans-Pacific propagation and warming effects of an El Niño anomaly. Nature 370:360–363.

Kindle, J. C., and P. A. Phoebus. 1995. Ocean response to operational westerly wind bursts during the 1991–92 El Niño. J. Geophys. Res. 100 C3:4893–4920.

Kousky, V. E., ed. 1989. Climate diagnostics bulletin, January 1989. Climate Analysis Center, National Meteorological Center, Washington, D.C. No. 89/1, 48 pp.

———. 1990. Climate diagnostics bulletin, January 1990. Climate Analysis Center, National Meteorological Center, Washington, D.C. No. 90/1, 53 pp.

Kumar, A., and M. P. Hoerling. 1995. Prospects and limitations of seasonal atmospheric GCM predictions. Bull. Am. Meteorol. Soc. 76:335–345.

Lau, K.-M., and H. Lim. 1984. On the dynamics of equatorial forcing of climate teleconnections. J. Atmos. Sci. 41:161–176.

Lynn, R. J., K. A. Bliss, and L. E. Eber. 1982. Vertical and horizontal distributions of seasonal mean temperature, salinity, sigma-t, stability, dynamic height, oxygen, and oxygen saturation in the California Current, 1850–1978. Calif. Coop. Oceanic Fish. Invest. Atlas 30. San Diego: Univ. Calif., 513 pp.

Lynn, R. J., F. B. Schwing, and T. L. Hayward. 1995. The effect of the 1991–1993 ENSO on the California Current system. Calif. Coop. Oceanic Fish. Invest. Rep. 36 (this volume).

Matsuno, T. 1966. Quasi-geostrophic motions in the equatorial area. J. Meteorol. Soc. Japan 44:25–42.

McPhaden, M. 1993. TOGA-TAO and the 1991–93 El Niño event. Oceanography 6:36–44.

Mysak, L. 1986. El Niño, interannual variability and fisheries in the northeast Pacific Ocean. Can. J. Fish. Aquat. Sci. 43:464–497.

Namias, J. 1986. Persistence of flow patterns over North America and adjacent ocean sectors. Monthly Weather Rev. 114:1368–1383.

Norton, J. G., and D. R. McClain. 1994. Diagnostic patterns of seasonal and interannual temperature variation off the west coast of the United States: local and remote large-scale atmospheric forcing. J. Geophys. Res. 99: 16,019–16,030.

Palmer, T. N., and D. A. Mansfield. 1986. A study of wintertime circulation anomalies during past El Niño events using a high resolution general circulation model. II: Variability of the seasonal response. Quart. J. Royal Meteorol. Soc. 112:639–660.

Pares-Sierra, A., and J. J. O'Brien. 1989. The seasonal and interannual variability of the California Current system: a numerical model. J. Geophys. Res. 94:3159–3180.

Peixoto, J. P., and A. H. Oort. 1992. Physics of climate. New York: American Institute of Physics, 520 pp.

Philander, G. S. 1990. El Niño, La Niña, and the Southern Oscillation. San Diego: Academic Press, 293 pp.

———. 1992. Ocean-atmosphere interactions in the tropics: a review of recent theories and models. J. Applied Meteorol. 31:938–945.

Quinn, R. K., D. O. Zopf, K. S. Short, and R. T. W. Kuo Yang. 1978. Historical trends and statistics of the Southern Oscillation, El Niño, and Indonesian droughts. Fish. Bull. 76:663–678.

Rassmusson, E. M., and T. H. Carpenter. 1982. Variations in tropical sea surface temperature and surface wind fields associated with the Southern Oscillation/El Niño. Monthly Weather Rev. 110:354–384.

Rienecker, M. M., and C. N. K. Mooers. 1986. The 1982–1983 El Niño signal off northern California. J. Geophys. Res. 91:6597–6608.

Simpson, J. J. 1992. Response of the southern California Current system to the mid-latitude North Pacific coastal warming events of 1982–1983 and 1940–1941. Fish. Oceanogr. 1:57–79.

Strub, P. T., and C. James. 1995. The large-scale summer circulation of the California Current. Geophys. Res. Lett. 22:207–210.

Tribbia, J. J. 1991. The rudimentary theory of atmospheric teleconnections associated with ENSO. *In* Teleconnections linking worldwide climate anomalies: scientific basis and societal impacts, M. H. Glantz, R. W. Katz, and N. Nicholls, eds. New York: Cambridge Univ. Press, 535 pp.

Wallace, J. M., and D. S. Gutzler. 1981. Teleconnections in the geopotential height field during the Northern Hemisphere winter. Monthly Weather Rev. 109:784–812.

White, W. B., Y. H. He, and S. E. Pazan. 1989. Off-equatorial westward propagating Rossby waves in the tropical Pacific during the 1982–83 and 1986–87 ENSO events. J. Phys. Oceanogr. 19:1397–1406.

Wooster, W. S., and D. L. Fluharty, eds. 1985. El Niño north. Seattle: Univ. Wash., 312 pp.

Wyrtki, K. 1989. February 1989 sea level. Climate diagnostics bulletin, March 1989. Climate Analysis Center, National Meteorological Center, Washington, D.C. No. 89/3:11–12.

———. 1992. February 1992 sea level. Climate diagnostics bulletin, March 1992. Climate Analysis Center, National Meteorological Center, Washington, D.C. No. 92/3:40–41.

———. 1993. February 1993 sea level. Climate diagnostics bulletin, March 1993. Climate Analysis Center, National Meteorological Center, Washington, D.C. No. 93/3:39–40.